

# We are IntechOpen, the world's leading publisher of Open Access books Built by scientists, for scientists

**4,800**

Open access books available

**122,000**

International authors and editors

**135M**

Downloads

Our authors are among the

**154**

Countries delivered to

**TOP 1%**

most cited scientists

**12.2%**

Contributors from top 500 universities



**WEB OF SCIENCE™**

Selection of our books indexed in the Book Citation Index  
in Web of Science™ Core Collection (BKCI)

Interested in publishing with us?  
Contact [book.department@intechopen.com](mailto:book.department@intechopen.com)

Numbers displayed above are based on latest data collected.

For more information visit [www.intechopen.com](http://www.intechopen.com)



# Single Photon Detection Using Frequency Up-Conversion with Pulse Pumping

Lijun Ma, Oliver Slattery and Xiao Tang

*Information Technology laboratory, National Institute of Standards and Technology  
United States of America*

## 1. Introduction

In any quantum communication system, such as a quantum key distribution (QKD) system, data rates are mainly limited by the system clock rate and the various link losses. While the transmission clock rate is limited by the temporal resolution of the single-photon detectors, losses in a fiber-based quantum communication system can be minimized by operating in the near infrared range (NIR), at 1310 nm or 1550 nm. Commercially available InGaAs-based avalanche photo-diodes (APDs) can be operated as single-photon detectors in this wavelength range [Hadfield, 2009]. Due to the severe after-pulsing, InGaAs APDs are typically used in a gated mode and this can limit their application in high-speed quantum communications systems. Superconducting single-photon detectors (SSPDs) can work in the NIR wavelength range with good performance [Gol'tsman et al. 2001; Hadfield, 2009]. However, SSPDs require cryogenic temperatures, and are not widely available on the commercial market at present. In addition, InGaAs/InP based photomultiplier tubes (PMT) can operate in the NIR range, but its performance is limited by very low detection efficiency (1 % at 1600 nm) and large timing jitter (1.5 ns) [Hamamatsu, 2005]. Microchannel plates (MCP) are micro-capillary electron multipliers coated with an electron-emissive material and multiply photon-excited electrons from a photon cathode [Wiza, 1979]. MCPs usually have faster rise times and lower timing jitter than is achievable with PMTs. InGaAs MCPs can work in the NIR range. These MCPs, but are limited by low detection efficiency (~1 %) [Martin, J. & Hink P. 2003].

On the other hand, silicon based avalanche photo-diodes (Si APDs) are compact, relatively inexpensive, and can be operated at ambient temperatures with high detection efficiency and low noise in the visible or near-visible range. Unfortunately they do not work at wavelengths longer than 1000 nm. For those wavelengths, an up-conversion technique has been developed that uses sum-frequency generation (SFG) in a non-linear optical medium to convert the signal photons to a higher frequency (shorter wavelength) in the visible or near visible range. The up-converted photons can then be detected by a Si APD. Up-conversion detectors use commercially available components and devices, and are a practical solution for many applications in quantum communications. To date, several groups have successfully developed highly efficient up-conversion single-photon detectors in the near-infrared range using periodically poled lithium niobate (PPLN) waveguides [Diamanti et al., 2005; Langrock et al., 2005; Thew et al., 2006; Tanzilli et al., 2005; Xu et al., 2007;] and bulk crystals [Vandevender & Kwiat, 2004].

Traditionally, an up-conversion single photon detector uses continuous wave (CW) pumping at a single wavelength. For a quantum communication system, a synchronized clock signal can be obtained from classical channels. Therefore, the up-conversion detector can be operated in pulsed pump mode using the synchronized clock signal. Up-conversion detectors with a pulsed pump can provide extra advantages that CW pumped detectors do not offer. For example, because the dark count rate in an up-conversion detector is dependent on the pump power, pulsed pump can significantly reduce the noise while keeping the same conversion efficiency. Furthermore, in the CW pump mode, the temporal resolution is determined by the timing jitter of the Si APD used in the detection system. The jitter-limited temporal resolution becomes a bottleneck as the transmission rate increases in a quantum communications system. An up-conversion single-photon detector using multiple spectrally and temporally distinct pulse pumps can support transmission rates significantly higher than the jitter-limited transmission rate of a traditional Si APD detector. In this chapter, we will describe in detail an up-conversion detector using a pulsed pump and its applications in noise reduction and transmission rate increase in quantum communication systems. This detector was developed at the National Institute of Standards and Technology.

## 2. Up-conversion detector with one wavelength pulsed pumping

### 2.1 Detector configuration

The configuration of an up-conversion detector with a single wavelength pulsed pump is shown in Fig. 1.

A 1550 nm CW laser provides the pump seed. The CW seed light is modulated to an optical pulse train by a Lithium Niobate-based electro-optical modulator (EO modulator). In many quantum information systems, the photons arrive with a synchronized classical signal. One can use the synchronized signal to modulate the pump seed resulting in the up-conversion detector operating a pulsed pump mode. This feature is similar to an optical gate, which is very useful for noise reduction or high speed gating in a communications system.

The modulated pump seed is then amplified by an erbium-doped fiber amplifier (EDFA). Two 1310/1550 wavelength division multiplexer (WDM) couplers with a 25 dB extinction ratio are used to suppress noise around 1310 nm at the output of the EDFA. The amplified pump light is then combined with a weak (single photon) signal in the 1310 nm range by another WDM coupler and the combined pump and signal are then coupled into the PPLN waveguides. The input polarization state of both the signal and the pump are adjusted by the polarization controllers, PC1 and PC2 respectively, before entering the coupler. The longer the waveguide length, the lower the pump power needed to reach the maximum conversion efficiency. The PPLN waveguide for the up-conversion detector is 5-cm long, the longest length possible using current manufacturing techniques. The input of the PPLN waveguide is fiber coupled, and the output is coupled into free-space through a 710 nm anti-reflection (AR) coating on the face of the waveguide. The output light of PPLN waveguide consists of a 710 nm (SFG) up-converted weak light signal, residual 1550 nm pump light and its second harmonic generation (SHG) light at 775 nm. These beams are separated by two dispersive prisms and the 710 nm photons are detected by a Si APD. An iris and a 20 nm band-pass filter are used to reduce other noise, such as external light leaked into the system.

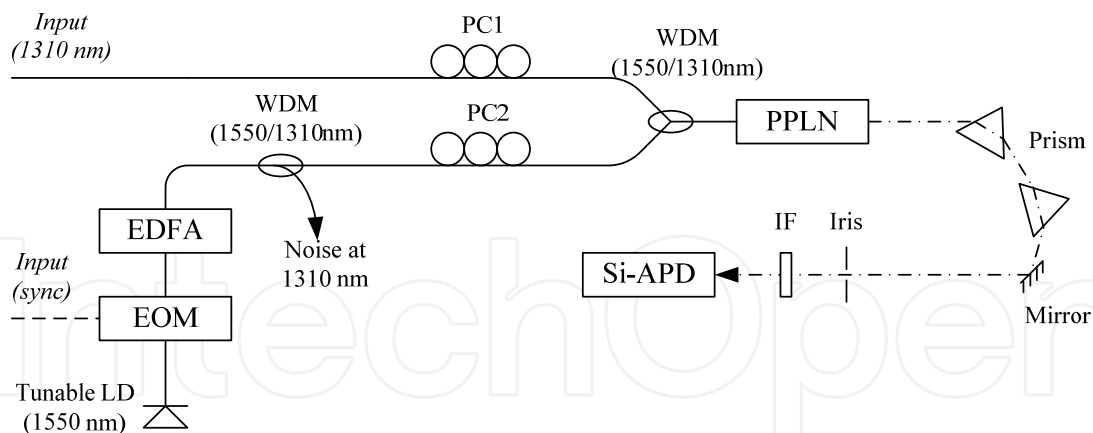


Fig. 1. Schematic diagram of an up-conversion detector with a pulsed pump. EOM: Electric-optic modulator; EDFA: Erbium-doped fiber amplifier; WDM: Wavelength-division multiplexing coupler; PC: Polarization controller; PPLN: Periodically-poled LiNbO<sub>3</sub> waveguides; IF: Interference filter. Solid line: Optical fiber; Dash line: Free space optical transmission.

## 2.2 Noise reduction in quantum communication systems

The noise, or dark counts, of a single photon detector is one of its important performance parameters: a higher dark count rate can cause more errors in the quantum information system and degrade the system's fidelity.

In an up-conversion single photon detector, the total dark counts originate from the intrinsic dark counts of the Si APD and the noise from the frequency conversion process inside the crystal. The intrinsic dark count rate is very low, and is usually negligible in comparison to the noise due to the frequency conversion process. It is widely believed that the noise which arises in the frequency conversion process stems from the spontaneous Raman scattering (SRS) [Diamanti et al., 2005; Langrock et al., 2005; Thew et al., 2006; Tanzilli et al., 2005; Xu et al., 2007; Vandevender & Kwiat, 2004] and spontaneous parametric down conversion (SPDC) [Pelc et al, 2010] generated in the waveguide by the strong pump. If these SRS photons or SPDC photons are generated at wavelengths within the signal band they can be up-converted to the detection wavelength, generating noise or 'dark' counts. In our experiment, we have shown that a pump using a longer wavelength than the signal avoids the SPDC photons leaving only the noise from the anti-Stokes photons of SRS.

The significance of the Raman scattering component can be estimated by first neglecting the SFG, loss, and pump depletion, and then solving the photon number for a given Stokes mode  $N_s$  using the differential equation of the Raman scattering [Smith, 1972] in a known length PPLN waveguide. The solution is given by

$$N_s = e^{g^L} - 1, \quad (1)$$

where the Raman gain,  $g$ , is given by  $\gamma P / A_{eff}$  and  $L$  represents the length. The quantity  $\gamma$  is the gain factor and the pump power,  $P$ , divided by the effective area,  $A_{eff}$ , gives the pump intensity.

In the above configuration, the 240-nm wavelength spacing between the pump (1550 nm) and the signal (1310 nm) is much larger than the peak Raman shift frequency of PPLN. Therefore,

$$e^{gL} - 1 \approx gL, \quad (2)$$

and the stimulated Raman scattering inside the PPLN is also negligible since a relatively low pump power is used. Therefore, we can assume that most of the Stokes photons are induced by the spontaneous Raman scattering inside the PPLN and this assumption enables a simple solution for the dark count.

The internal conversion efficiency ( $\eta_C$ ) in the PPLN waveguide is a function of pump power, and is determined by the following equation [Diamanti et al., 2005; Langrock et al., 2005; Thew et al., 2006; Tanzilli et al., 2005; Xu et al., 2007; Vandevender & Kwiat, 2004]:

$$\eta_C(P) = \eta_0 \sin^2 \left( k \sqrt{P / A_{eff}} \cdot L \right), \quad (3)$$

where  $\eta_0$  is the peak conversion efficiency.  $\eta_0$  is dependent on the quality of the PPLN waveguide and can reach 1 in a waveguide with high poling quality. The pump intensity is the ratio of the power,  $P$ , to the effective area,  $A_{eff}$ .  $L_{PPLN}$  is the PPLN waveguide length.  $k$  is a constant and determined by

$$k = \left( \frac{\omega_s \omega_p d_{eff}^2}{n_s n_p c^2} \right)^{1/2}, \quad (4)$$

where  $\omega_s$  and  $\omega_p$  are the signal and pump wavelengths;  $n_s$  and  $n_p$  are the refractive index of lithium niobate for the signal and pump wavelengths.  $d_{eff}$  represents the effective nonlinear coefficient and  $c$  is the speed of light.

Using the above assumptions in Eq. (1), one can get a differential equation for the Stokes photon:  $dN_s / dz = g = \gamma P / A_{eff}$  with  $z$  being a distance inside the PPLN waveguide from the input surface. A generated Stokes photon will be up-converted to the detection wavelength and induce a dark count. Consequently, by further applying the conversion efficiency of the PPLN, Eq. (3-4), we can write the dark count rate, DCR, as a function of pump power:

$$\begin{aligned} DCR_{Raman}(P) &= \eta_{APD} \eta_T \int_0^{L_{PPLN}} \frac{\gamma \times P}{A_{eff}} \sin^2 \left[ (L - z) k \sqrt{P / A_{eff}} \right] dz \\ &= \frac{\gamma}{2A_{eff}} \eta_{APD} \eta_T P L_{PPLN} \left[ 1 - \frac{\sin \left( 2k \sqrt{P / A_{eff}} L \right)}{2k \sqrt{P / A_{eff}} L} \right], \end{aligned} \quad (5)$$

where  $\eta_T$  is the overall transmission efficiency and  $\eta_{APD}$  is the detection efficiency of the Si APD. The linear term of the pump power,  $P$ , in the integral describes the generation of Stokes photons via the spontaneous Raman scattering and the sinusoidal term describes the up-conversion of the Stokes photons generated at  $z$  contributing to a dark count at the PPLN output ( $z = L$ ). In the above derivation, we also neglected the optical loss in the PPLN waveguide. This assumption is justified by the fact that low waveguide loss is achieved with current manufacturing techniques and nearly 100 % internal conversion efficiency has been reported.

From the above analyses, one can see the conversion efficiency and noise both are dependent on the pump power. In a quantum communication system, each time bin is usually much longer than the optical pulse, because the single photon detectors have large timing jitter. When the pump pulse width is larger than the optical signal width, the photons can be converted at the highest efficiency. By turning off the pump after the signal pulse the dark counts rate can be reduced. When the pump is off, Si-APDs and counting board still operate, so the counts triggered by the signal photons delayed by the detector's jitter can still be recorded. In that case, we can reduce the noise while the efficiency is not affected.

We have experimentally demonstrated the up-conversion detector with a pulsed pump. The conversion efficiency as the function of pump power is shown in Fig. 2. The detection efficiency measured here is from a 625 MHz synchronized signal with 600 ps (FWHM) pump pulses. The optical pulse is pumped with the same synchronized signal but has a shorter (300 ps FWHM) pulse width. The detector operating in pulsed pump mode can reach the maximum conversion efficiency with a lower average pump power, which helps to reduce noise. The optimal pump powers (average) are 38 mW and 78 mW, for the pulsed and CW pump modes respectively.

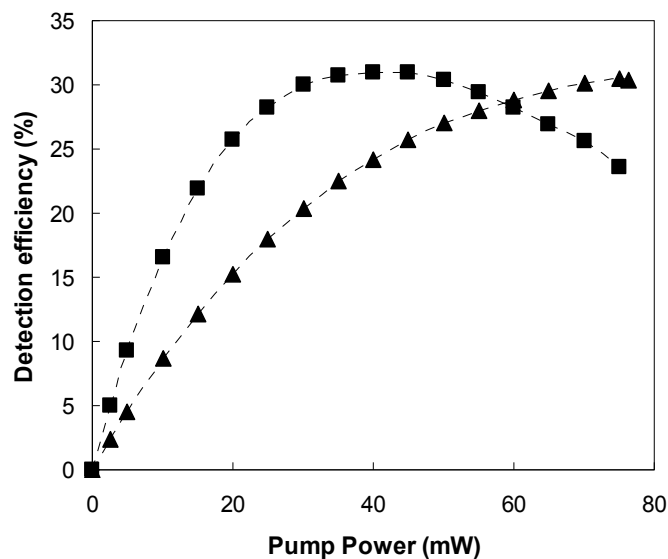


Fig. 2. The detection efficiency as a function of pump power. Two cases are studied: CW pump (triangle) and pulsed pump (square).

As shown in the Fig. 3, the pulsed pump generates more dark counts than the CW pump for a given average power since the peak power of the pulsed pump is higher than the average power. However, the pulsed pump needs less average power than the CW pump to achieve a given detection efficiency. Therefore, the pulse pump can achieve a given detection efficiency with less dark counts in comparison to the CW pump. For example, the maximum detection efficiency is reached when using the pulsed pump at 38 mW and the dark count rate is 2400 c/s. For the CW pump, a power of 78 mW is needed to achieve the maximum detection efficiency, which incurs a dark count rate of 3100 c/s. Consequently, a pulsed pump needs lower average power and effectively reduces the dark count rate compared to a CW pump.

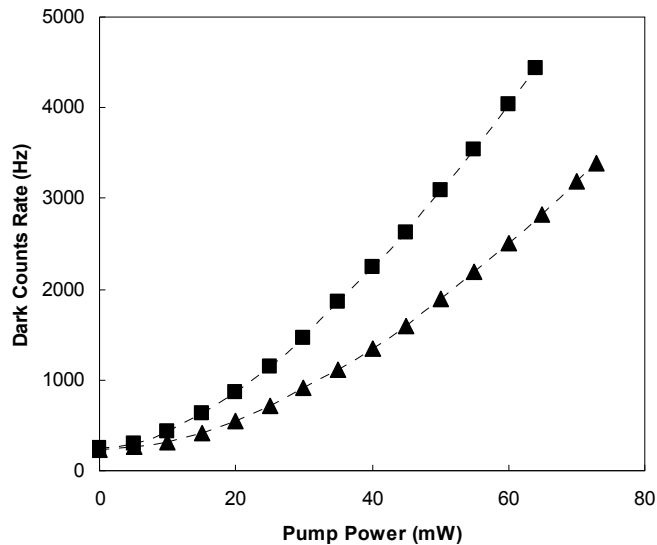


Fig. 3. The dark count rate as a function of average pump power at the PPLN input. Two cases are studied: CW pump (triangle) and pulsed pump (square).

To demonstrate the performance of the above up-conversion detector with pulsed pumping, we integrated them into one of our QKD system [Xu et al., 2007]. The quantum keys are encoded by photons in the quantum channel at 1310 nm using the B92 protocol [Bennett, 1992], as shown in Fig. 4. The QKD system uses a custom printed circuit board with a field-programmable gate array (FPGA) [Mink et al. 2006; Mink et al. 2009] to generate a random stream of quantum data for the photons and to transmit and receive the classical data. The classical data is carried by the optical signal in the classical channel at 1550 nm. To polarization-encode the quantum channel with the random quantum data, we first modulate a 1310-nm CW light into a 625 MHz pulse train, which is evenly split into two polarization channels. Each pulse train is further modulated by one of two complementary 625 Mbit/s quantum channel data streams. The two quantum channels are combined by a 45-degree polarization-maintaining combiner and attenuated to a mean photon number of 0.1 per bit, and then multiplexed with the classical channel and sent to a standard single-mode fiber. At Bob, another WDM is used to demultiplex the quantum and classical channels. The quantum channel is polarization-decoded and detected using the up-conversion single-photon detectors, and the detection events are recorded to generate raw keys. Bob's board informs Alice of the location of the detection events via the classical channel. After reconciliation and error correction, Alice and Bob obtain a common version of shared secret key bits, which are further used to encode and decode information for secure communication between Alice and Bob.

The system performance is shown in Fig. 5. During our measurements, the pump power was fixed at 40 mW. The sifted-key rate is 2.5 Mbit/s for a back-to-back connection, 1 Mbit/s at 10 km, and 60 Kbit/s at 50 km. The quantum bit error rate (QBER) is approximately 3% for the back-to-back configuration, remains below 4% up to 20 km, and reaches 8% at 50 km. The finite extinction ratio of the modulator and the system timing jitter induce a background QBER of approximately 2.5% and the rest is from dark counts generated by both the pump light and the classical channel. We also calculated the theoretical sifted-key rate and QBER and they agree well with the measured results.

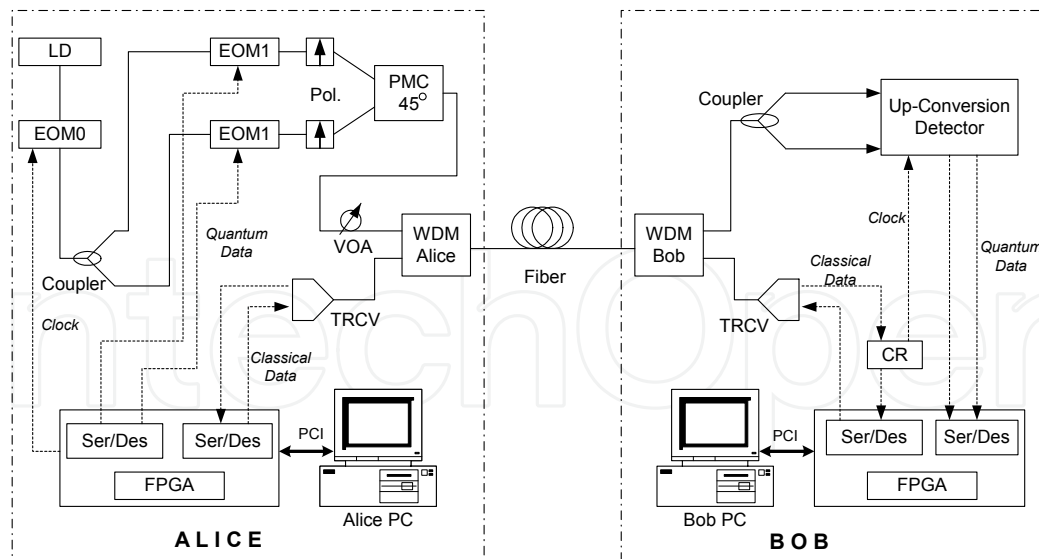


Fig. 4. The B92 polarization coding QKD system. LD: Laser diode; EOM: Electric-optic modulator (LiNbO<sub>3</sub>); PC: Polarization controller; PMC-45°: Polarization maintaining combiner that combines two light signals that are separated by 45 degrees; VOA: Variable optical attenuator; WDM: Wavelength-division multiplexer; SMF: Standard single-mode fiber; TRCV: Optical transceiver; CR: Clock recovery module; FPGA: Custom printed circuit board controlled by a field-programmable gate array; PCI: PCI connection; Dotted line: Electric cable; Solid line: Optical fiber.

Although the pump power is fixed near the optimal value for maximum up-conversion efficiency, the QBER remains small until the distance reaches close to 20 km due to the low dark count rate caused by the 1550 nm up-conversion detector. This QKD system can generate secure keys in real time for one-time-pad encryption and decryption of a continuous 200 Kbit/s video transmission stream over 10 km fiber. The system performance demonstrates that the up-conversion detectors with pulse pumping are suitable for the fiber-based polarization-encoding QKD system, realizing high speed secured data transmission.

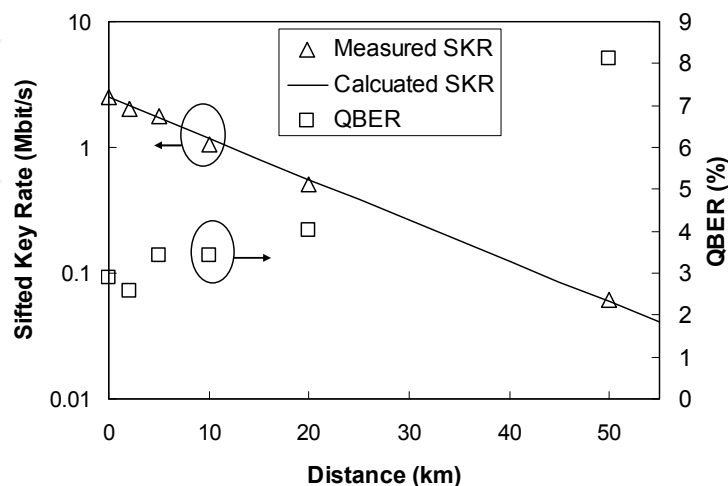


Fig. 5. The system performance of the B92 polarization-based QKD system using pulsed pump up-conversion detectors.

### 3. Up-conversion detector with multiple wavelength pulse pumping

#### 3.1 The scheme and detector configuration

In many recent quantum communication systems, the photon sources can generate and temporally encode data at rates significantly higher than what single-photon detectors can resolve. For example, commercially available mode-locked lasers or optical modulators can generate sub-10 ps optical pulses, and broadband SPDC sources can readily prepare optical states of photon pairs with sub-100 fs correlation time. On the other hand, current high-resolution single-photon detectors exhibit a FWHM temporal resolution of the order of 50 ps. In a quantum communication system, insufficient temporal resolution in the detector can cause inter-symbol interference (ISI), i.e., a detection signal can be recorded at a time slot adjacent to the intended one, and this can induce a significant error rate. The transmission rate is therefore limited by the temporal resolution of the single-photon detectors. As a figure of merit, a single-photon signal can be received with an acceptable error rate when the transmission period is equal to or larger than the full width at 1% of the maximum (FW1%M) of the single-photon detector's response histogram [Restelli et al. 2009]. For most types of Si APDs the FW1%M is significantly larger than the commonly cited FWHM. At the peak of a typical Si APD's response histogram, where the FWHM is measured, the profile is approximately Gaussian. However, at lower part of the detector's response curve, the response histogram profile deviates significantly from Gaussian, often exhibiting a long exponential tail, which dramatically increases the FW1%M of the device. A typical commercially-available Si APD has a FWHM of about 350 ps, but a FW1%M of about 1100 ps that limits the transmission rate to less than 1 GHz for a quantum communication system using an up-conversion detector equipped with this type of Si APD.

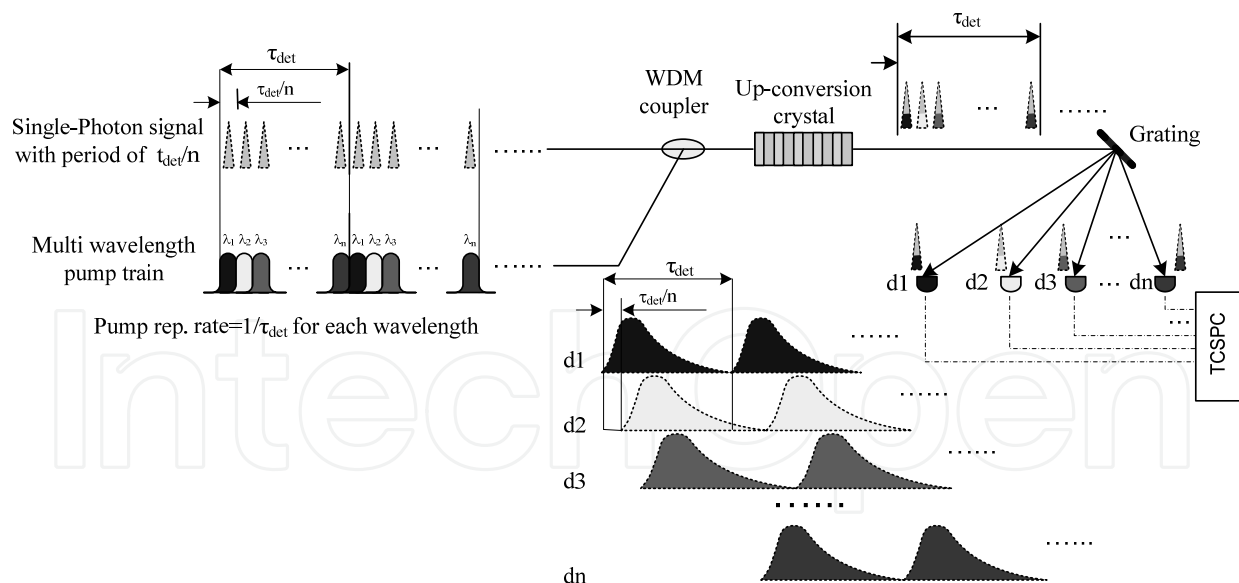


Fig. 6. Schematic diagram of up-conversion single-photon detection with multi-wavelength optical sampling. A sequence of  $n$  spectrally and temporally distinct pump pulses are used to sub-divide the minimum resolvable time bin,  $\tau_{det}$ , of conventional Si APDs, increasing the temporal resolution of the overall system by a factor of  $n$ . The incident single-photon signal is combined with the sequence of pump pulses with a wavelength division multiplexer (WDM). Detection events from each of the  $n$  Si APDs are time-tagged with time-correlated single-photon counting (TCSPC).

To increase the temporal resolution of an up-conversion detection system beyond that of its constituent Si APDs, a sequence of spectrally and temporally distinct pump pulses can be used to sub-divide the minimum resolvable time period  $\tau_{det}$ . This application of optical sampling is illustrated in Fig. 6, where  $n$  pump pulses with different wavelengths are used to sample the incident single-photon signal in intervals of duration  $\tau_{det}/n$ . To ensure optimum detection efficiency, each pump pulse is wider than the single-photon signal pulses. The repetition rate for each particular wavelength of the pump is  $1/\tau_{det}$ . When a signal photon enters and co-propagates with one of the strong pump pulses in a quasi-phase matched sum-frequency device, such as PPLN, it can be up-converted to the visible range. The specific wavelength of the up-converted photon is determined by the wavelength of the pump pulse with which it interacted. A subsequent dispersive element such as a grating can separate the up-converted signal photons and distribute them to an array of Si APDs. Each Si APD in the array therefore corresponds to a particular pump wavelength, and, by extension, a particular arrival time period of duration  $\tau_{det}/n$ . In such a configuration the sampling period for each Si APD is  $\tau_{det}$ , allowing it to accurately resolve the signal without ambiguity due to the detector's temporal response. With this approach, the detection system is able to resolve the single-photon signal in a period as small as  $\tau_{det}/n$ , representing an increase in temporal resolution by a factor of  $n$ .

The experimental configuration of an up-conversion detector with a multiple wavelength pulse pump is shown in Fig. 7. A pattern generator drives the pulse-carving systems for the two up-conversion pump sources at 1549.2 nm and 1550.0 nm. Each pump source has a period of 1.25 ns. Before the pump and the signal are combined the pulses from the first pump are aligned with the odd signal pulses, and the pulses in the second pump are aligned

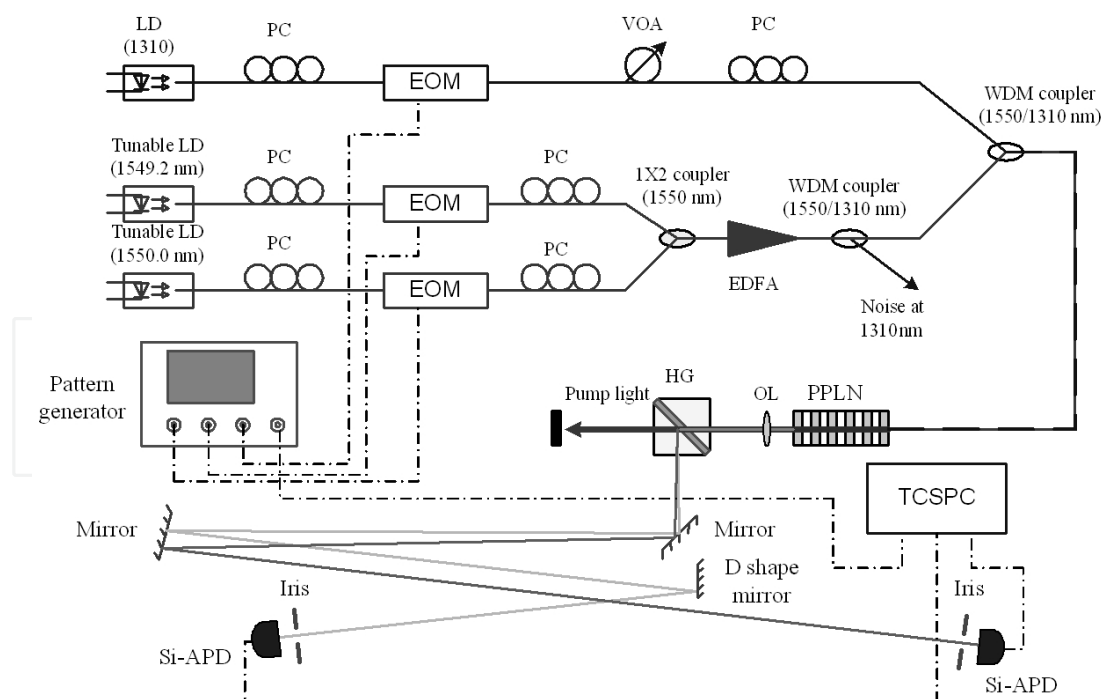


Fig. 7. Experimental setup. LD: Laser Diode, EOM: Electric-optic Modulator; EDFA: Erbium-doped fiber amplifier; WDM: Wavelength-division multiplexing coupler; PC: Polarization controller; PPLN: Periodically-poled LiNbO<sub>3</sub> waveguides; OL, Objective Lens; HG, Holographic Grating. TCSPC: time-correlated single photon counting;

with the even signal pulses by adjusting the delays in the pattern generator, as shown in Fig. 8. The pump-pulse duration used in the experiment is 400 ps, which is wider than the 220 ps signal pulse and chosen to provide higher conversion efficiency [Xu et al., 2007]. The two pump beams are combined by a 1x2 coupler and then amplified by a 1-Watt EDFA. At the output of the EDFA, two 1310/1550 WDM couplers are used in series, giving a 50-dB extinction ratio in total, to suppress noise around 1310 nm. The amplified pump light is then combined with the 1310-nm signal by another WDM coupler, and the combined pump and signal are coupled into the up-conversion medium. Up-conversion takes place in a 1-cm PPLN waveguide that has a fiber-coupled input and a free-space output. When mixed with the slightly different pump wavelengths in the PPLN waveguide, the 1310 nm signal photons are up-converted to output photons at 710.0 nm and 709.8 nm. The output beam is filtered to remove noise and excess pump light and then diffracted by a holographic grating. After a 3-m long path the 710.0 nm and 709.8 nm photons are sufficiently separated that they can be directed onto two Si APDs. In this system an adjustable iris placed in front of the Si APD, in conjunction with the holographic grating, act as a 0.4-nm band-pass filter, which greatly reduces the dark count rate. The detected signals are then counted by a time-correlated single photon counting system.

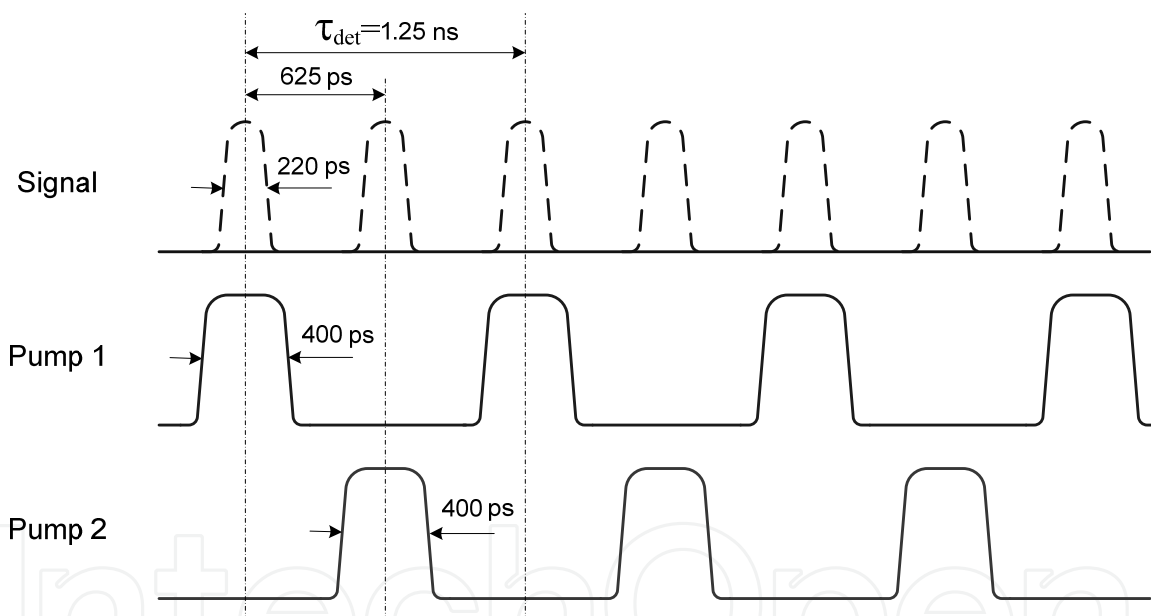


Fig. 8. Timing diagram of the signal, pump 1 and pump 2 used in the multi-wavelength optical sampling single-photon detection system.

In this experiment we use a 1-cm long PPLN waveguide. A shorter waveguide provides a broader spectral bandwidth, which is necessary to cover the spectral separation of the two output photons. In the previously described work, we have demonstrated high single-photon up-conversion efficiency with a longer 5-cm PPLN waveguide, but we find that the quasi-phase matched bandwidth for such a waveguide is too narrow for the current approach. The transfer function response of a finite-length uniform quasi-phase matching grating is [Fejer et al. 1992]:

$$I_{SFG}(\Delta k) \propto I_{pump} \cdot I_{signal} \cdot \text{sinc}^2(\Delta k \cdot L / 2), \quad (6)$$

where  $I_{SFG}$ ,  $I_{pump}$ , and  $I_{signal}$  are the intensities of SFG, pump, and signal light, respectively,  $L$  is the waveguide length, and  $\Delta k$  is the phase-mismatching, which determines the bandwidth of the spectral response. According to Eq. (6), for a given SFG intensity, the waveguide length and the spectral response bandwidth are inversely proportional; the shorter the waveguide, the broader the spectral response bandwidth. Fig. 9 (a) shows the spectral response measured experimentally for the 1-cm PPLN waveguide. Its 3-dB bandwidth is about 1.3 nm, which is about 5 times wider than that of the 5-cm PPLN waveguide (0.25 nm) [Ma et al. 2009]. In this experiment the wider bandwidth allows two pumps, at wavelengths 1549.2 nm and 1550.0 nm, to operate with almost the same conversion efficiency, which is about 85% of the maximum conversion efficiency.

Detection efficiency is a significant trade off for a short waveguide. From Eq. (3), to compensate for the reduced conversion efficiency in a shorter waveguide the pump power must be scaled quadratically. For example, the pump power required to achieve the maximum conversion efficiency in a 1-cm waveguide is 25 times higher than that for a 5-cm waveguide. Fig. 9(b) shows the detection efficiency of the up-conversion detector as a function of the average pump power. The pump power on the x-axis is measured at the input fiber of the PPLN waveguide. Although the maximum output power of the EDFA is 1 W, the maximum power at the input fiber is approximately 510 mW due to losses in the WDM couplers and connectors between the EDFA and the waveguide. In our system the combined pulse duration of the two pumps covers 67% of each clock period, and therefore the peak power of each pulse is only 1.5 times higher than the average power. Fig. 9(b) indicates that the up-conversion efficiency of the detector does not reach its potential maximum value and is limited by the available pump power. Besides the insufficient pump power, the detection efficiency in our system is further reduced by the absence of an AR coating on the waveguide ends, causing about 26% loss, and, as stated above, the fact that the two pumps operate at wavelengths that provide 85% of the peak spectral response. Due to these factors, the overall detection efficiency is measured to be 7 %. The detection efficiency can be improved by using a higher pump power and an AR-coated waveguide. Selecting pump wavelengths closer to the center of spectral response can also improve the overall detection efficiency, but this puts more stringent demands on the spectral separation before the Si APDs.

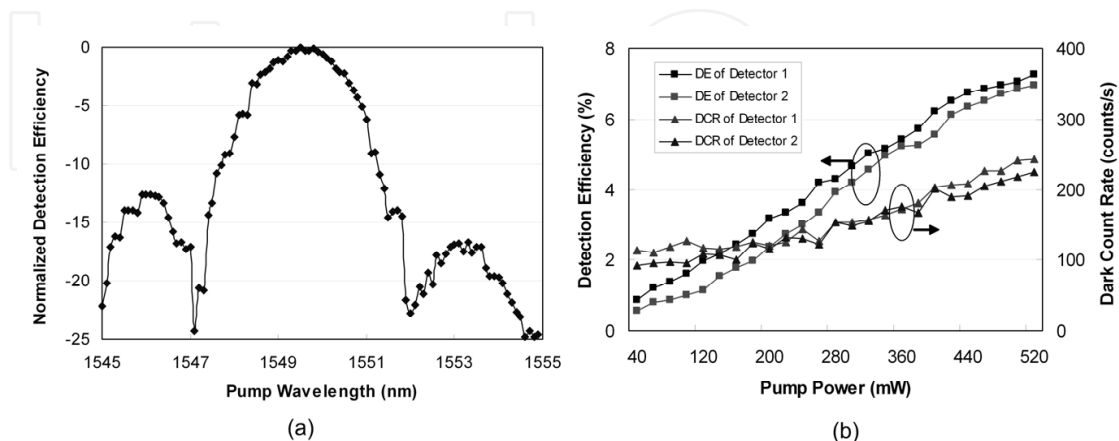


Fig. 9. (a) The spectral efficiency of the up-conversion detector. (b) The detection efficiency (DE) and dark count rate (DCR) as function of pump power. The pump power is measured in the input fiber of the PPLN waveguide.

Similar to other single photon detectors, the dark counts of this detector is caused by the anti-Stokes components of SRS in this waveguide and the intrinsic dark counts of Si APD. The SRS photons are generated over a broad spectrum, while the up-converted signal can be quite narrow. To further reduce the noise count rate, it is beneficial to use a bandpass filter with a very narrow bandwidth behind the waveguide. As stated above, in this experiment the iris in front of the Si APDs and the holographic grating constitute a band-pass filter with a bandwidth of about 0.4 nm. From Fig. 9 (b), the total dark count rate of the two Si APDs in the up-conversion detector are approximately 240 and 220 counts per second, respectively, at the maximum pump power.

### 3.2 Increasing transmission rate of a communication system

For a quantum communication system, inter-symbol interference (ISI) can be a significant source of errors. ISI can be caused by timing jitter of single photon detectors, and to avoid a high bit-error rate, the transmission data cycle should be equal to or larger than the FW1%M of the response histogram. For the 220-ps signal pulse used in our system, the response histogram of an up-conversion detector with a single wavelength pump is shown in Fig. 10 (black). The FW1%M of the histogram is about 1.25 ns and this detection system can therefore support a transmission rate of 800 MHz. When such a detection system is used to detect a 1.6 GHz signal, the insufficient temporal resolution of the detector results in severe ISI, as indicated by the poor pulse resolution, shown in Fig. 10 (grey). The application of optical sampling with two spectrally and temporally distinct pump pulses and a separate Si APD for each pump wavelength, as described above, accommodates the 1.25-ns FW1%M of each individual pump channel but supports an overall transmission rate of 1.6 GHz with low ISI. Fig. 11 (a) show the response histogram of each APD in the optical-sampling up-conversion system for a repetitive signal pattern “11111111”. For each APD, the detection window is larger than FW1%M of APD response, so the ISI is greatly diminished. To illustrate both the temporal demultiplexing and the ISI in this system, Fig. 11 (b) shows the response histogram of each of the two APDs for a repetitive signal pattern “10010110”. The

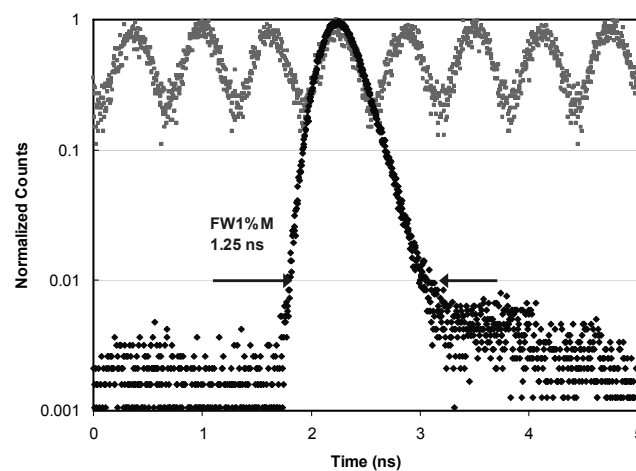


Fig. 10. Response histogram of the up-conversion detector with a single pump wavelength. The response histogram of single pulse (black) shows the FW1%M is 1.25 ns and its temporal resolution is insufficient to resolve, with low ISI, the repetitive data pattern “11111111” at 1.6 GHz (grey).

APD 1 receives the signal at odd time bins, resulting in the pattern "1001" and APD 2 receives the signal at even time bins resulting in the pattern "0110", and the original signal can be reconstructed from the data recorded by the two APDs. To measure the ISI in the optical sampling up-conversion system under conditions found in a typical QKD system we also drove the signal with a 1.6 Gb/s pseudo-random data pattern. After comparing the received data to the original data, the error rate was found to be approximately 1.2%. Subtracting the error rate caused by the imperfect extinction ratio of the modulator and the intrinsic dark counts of APDs, the error rate caused by ISI is less than 1%.

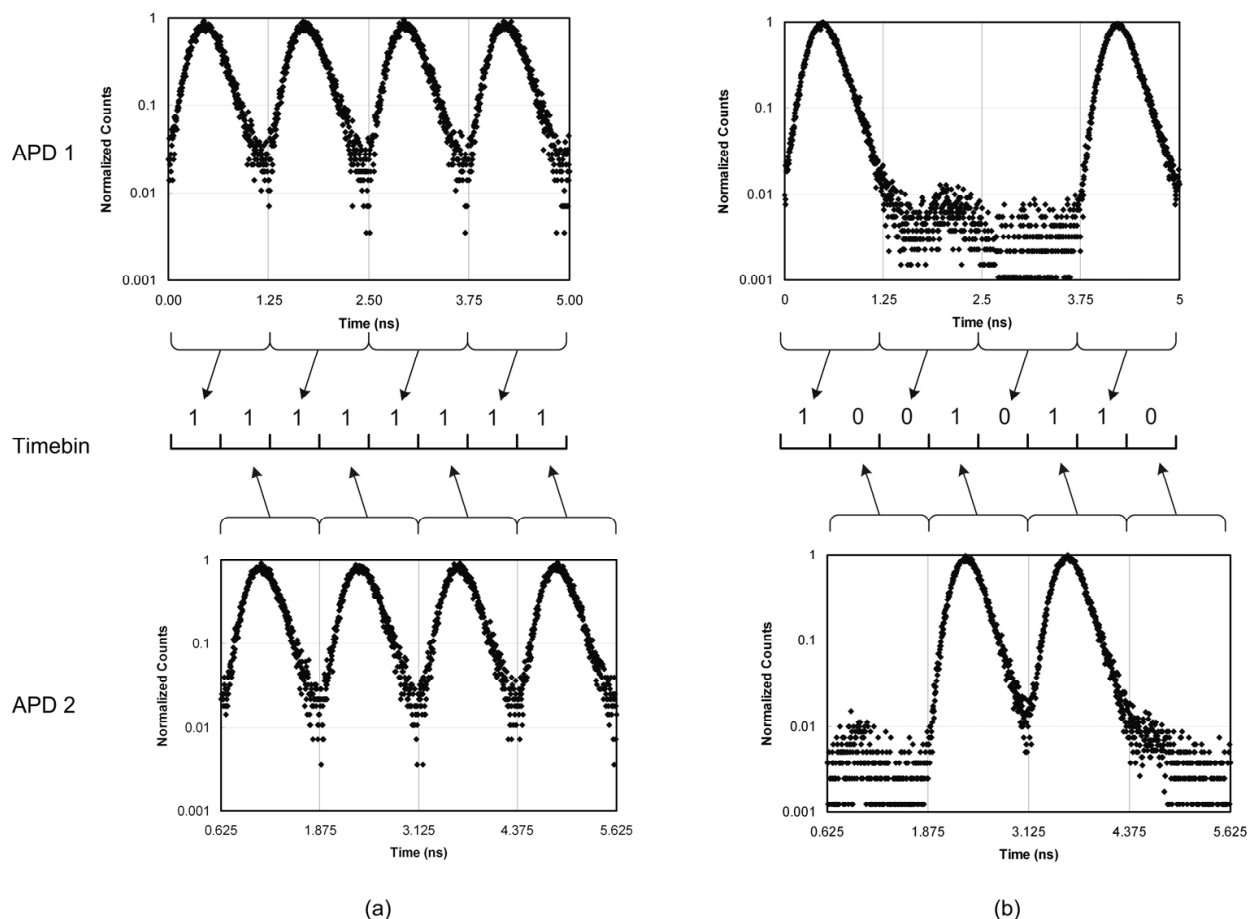


Fig. 11. Response histogram of the up-conversion detector with two spectrally and temporally distinct pump pulses (a) response histogram of APD 1 and APD 2, for a repetitive signal pattern "1111111" at 1.6 GHz. (b) response histogram of APD 1 and APD 2, for a repetitive data pattern 10010110 at 1.6 GHz.

The above experimental results demonstrate that an up-conversion single-photon detector with two spectrally and temporally distinct pump pulses can operate at transmission rates that are twice as fast as can be supported by its constituent APDs. Further sub-division of the APD's minimum resolvable period (e.g. the FW1%M) is possible with more pump wavelengths and a corresponding number of Si APDs, allowing further increases in the maximum supported transmission rate of the single-photon system. However, the ability to increase the temporal resolution is ultimately limited by the phase-matching bandwidth of the nonlinear waveguide and available pump power.

Fourier analysis shows that shorter pulse duration corresponds to a broader frequency bandwidth. Considering only transform limited Gaussian pulses, the relationship between the pulse duration and spectral bandwidth for such “minimum uncertainty” pulses is given by [Donnelly and Grossman, 1998]:

$$t_{FWHM} \cdot \omega_{FWHM} = 4\ln(2), \quad (6)$$

where  $t_{FWHM}$  and  $\omega_{FWHM}$  are the FWHM of temporal width and frequency bandwidth, respectively. For the pump wavelengths in our experiment (~1550 nm), pulse widths shorter than 3 ps correspond to frequency bandwidths larger than 1.2 nm, which covers most of the 3-dB quasi-phase matching bandwidth of our 1-cm PPLN waveguide and thus precludes any other up-conversion pump wavelengths. A 100-ps pump pulse corresponds to a transform-limited bandwidth of 0.035 nm, in which case the waveguide used in our experiment could support more than 10 pump channels with greater than 50% quasi-phase matching efficiency. In this case, its temporal resolution can be increased by one order-of-magnitude compared to an up-conversion detector with just one pump wavelength. To provide uniform detection efficiency across all temporal regions, the pump power can be reduced in the well-phase-matched regions to match the conversion efficiency in the outlying spectral regions.

As the pump wavelengths become closer together, or if a shorter nonlinear waveguide is used to increase the quasi-phase matching bandwidth, technical issues associated with obtaining high optical powers in each pump, and efficient spectral separation of the up-converted photons become significant. We note that novel nonlinear crystal structures, such as chirped gratings or adiabatic gratings [Suchowski et al. (2010)] can provide broad bandwidth and relatively high conversion efficiency. With these new technologies, we believe it is reasonable to consider an up-conversion single-photon detector using spectrally and temporally distinct pump pulses with temporal resolution better than 10 ps. It should be noted that this scheme is not only suitable for up-conversion detectors using Si APDs; other single-photon detectors with better temporal resolution, such as SSPDs, can also be integrated into the scheme for further improvement of their temporal resolution.

#### 4. Conclusion

Frequency up-conversion single photon detector technology is an efficient detection approach for quantum communication systems at NIR range. Traditionally, an up-conversion single photon detector uses CW pumping at a single wavelength. In CW pump mode, the pump power is usually set at a level where the conversion efficiency is the highest. In that case, the noise counts caused by the SRS in the waveguide might induce high error rates in a quantum communication system. An up-conversion single photon detector with a pulsed pump can reduce the noise count rate while maintaining the conversion efficiency. Furthermore, in a CW pump mode, the temporal resolution is determined by the timing jitter of the Si APD used in the detection system. A multiple wavelength pumping technique adds a new wavelength domain into the upconversion process. The data detected within a period of the Si APD's time jitter can be projected into the wavelength domain so that the spectrally and temporally distinct pulse pumping increases both the temporal resolution and the system data transmission rate.

## 5. Acknowledgement

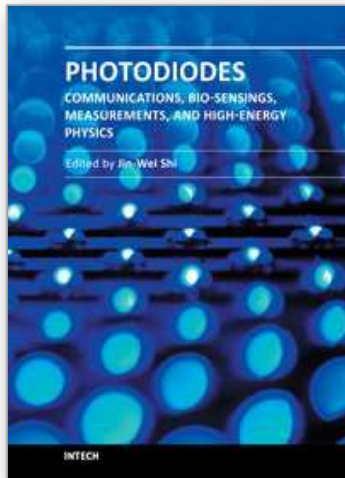
The authors would like to thank for the support from NIST Quantum Information Initiative. The authors also thank Dr. Alan Mink, Dr. Joshua C. Bienfang and Barry Hershman for their supports and discussions.

## 6. References

- Bennett, C. H. (1992). Quantum cryptography using any two nonorthogonal states. *Phys. Rev. Lett.*, Vol. 68, pp 3121-3124
- Diamanti, E.; Takesue, H.; Honjo, T.; Inoue, K. & Yamamoto, Y. (2005). Performance of various quantum-key-distribution systems using 1.55- $\mu\text{m}$  up-conversion single-photon detectors. *Phys. Rev. A*, Vol. 72, 052311
- Donnelly, T. D. and Grossman, C. (1998) Ultrafast phenomena: A laboratory experiment for undergraduates. *Am. J. Phys.* Vol. 66, pp 677-685
- Fejer, M.; Magel, G.; Jundt, D. & Byer, R. (1992). Quasi-phase-matched second harmonic generation: tuning and tolerances. *IEEE J. Quantum Electron.* Vol.28, pp 2631-2654
- Gol'tsman, G. N.; Okunev, O.; Chulkova G.; Lipatov, A.; Semenov, A.; Smirnov, K.; Voronov, B. & Dzardanov, A. (2001). Picosecond superconducting single-photon optical detector. *Appl. Phys. Lett.* Vol. 79, pp 705-707
- Hadfield, R. (2009). Single-photon detectors for optical quantum information applications, *Nat. Photonics*, Vol. 3, pp 696-705
- Hamamatsu. (2005). Near infrared photomultiplier tube R5509-73 data sheet.
- Langrock, C.; Diamanti, E.; Roussev, R. V.; Yamamoto, Y.; Fejer, M. M. & Takesue, H. (2005). Highly efficient single-photon detection at communication wavelengths by use of upconversion in reverse-proton-exchanged periodically poled LiNbO<sub>3</sub> waveguides. *Opt. Lett.* Vol. 30, pp. 1725-1727
- Ma, L., Slattery, O. and Tang, X. (2009) Experimental study of high sensitivity infrared spectrometer with waveguide-based up-conversion detector. *Opt. Express* Vol 17, pp 14395-14404.
- Martin, J. & Hink P. (2003) Single-Photon Detection with MicroChannel Plate Based Photo Multiplier Tubes. *Workshop on Single-Photon: Detectors, Applications and Measurement Methods, NIST.*
- Mink, A.; Tang, X.; Ma, L.; Nakassis, T.; Hershman, B.; Bienfang, J. C.; Su, D.; Boisvert, R.; Clark, C. W. & Williams, C. J. (2006). High speed quantum key distribution system supports one-time pad encryption of real-time video. *Proc. of SPIE*, Vol. 6244, 62440M,
- Mink, A., Bienfang, J., Carpenter, R., Ma, L., Hershman, B., Restelli, A. and Tang, X. (2009) Programmable Instrumentation & GHz signaling for quantum communication systems. *N. J. Physics*, Vol. 11: 054016,
- Pelc, J. S., Langrock, C., Zhang, Q. and Fejer, M. M. (2010) Influence of domain disorder on parametric noise in quasi-phase-matched quantum frequency converters. *Opt. Lett.*, Vol. 35, pp 2804-2806
- Restelli, A., Bienfang, J. C., Mink, A. and Clark, C. (2009) Quantum key distribution at GHz transmission rates. *Proc. of SPIE* Vol. 7236, 72360L,
- Smith, R. G. (1972) Optical power handling capacity of low loss optical fibers as determined by stimulated Raman and Brillouin scattering. *Appl. Opt.* Vol. 11, pp. 2489-2494

- Suchowski, H., Bruner, B. D., Arie, A. and Silberberg, Y. (2010) Broadband nonlinear frequency conversion. *OPN* Vol. 21, pp 36-41
- Tanzilli, S.; Tittel, W.; Halder, M.; Alibart, O.; Baldi, P.; Gisin, N. & Zbinden, H. (2005). A photonic quantum information interface. *Nature*, Vol 437, pp 116-120
- Thew, R. T.; Tanzilli, S.; Krainer, L.; Zeller, S. C.; Rochas, A.; Rech, I.; Cova, S.; Zbinden, H. & Gisin, N. (2006). Low jitter up-conversion detectors for telecom wavelength GHz QKD. *New J. Phys.* Vol. 8, pp 32.
- Vandevender, A. P. & Kwiat, P. G. (2004). High efficiency single photon detection via frequency up-conversion. *J. Mod. Opt.*, Vol. 51, 1433-1445
- Wiza, J. (1979). Microchannel plate detectors. *Nuclear Instruments and Methods* Vol. 162: pp 587-601
- Xu, H.; Ma, L.; Mink, A.; Hershman, B. & Tang, X. (2007). 1310-nm quantum key distribution system with up-conversion pump wavelength at 1550 nm. *Optics Express*, Vol 15, No.12, pp 7247- 7260

IntechOpen



## **Photodiodes - Communications, Bio-Sensings, Measurements and High-Energy Physics**

Edited by Associate Professor Jin-Wei Shi

ISBN 978-953-307-277-7

Hard cover, 284 pages

**Publisher** InTech

**Published online** 06, September, 2011

**Published in print edition** September, 2011

This book describes different kinds of photodiodes for applications in high-speed data communication, biomedical sensing, high-speed measurement, UV-light detection, and high energy physics. The photodiodes discussed are composed of several different semiconductor materials, such as InP, SiC, and Si, which cover an extremely wide optical wavelength regime ranging from infrared light to X-ray, making the suitable for diversified applications. Several interesting and unique topics were discussed including: the operation of high-speed photodiodes at low-temperature for super-conducting electronics, photodiodes for bio-medical imaging, single photon detection, photodiodes for the applications in nuclear physics, and for UV-light detection.

### **How to reference**

In order to correctly reference this scholarly work, feel free to copy and paste the following:

Lijun Ma, Oliver Slattery and Xiao Tang (2011). Single Photon Detection Using Frequency Up-Conversion with Pulse Pumping, Photodiodes - Communications, Bio-Sensings, Measurements and High-Energy Physics, Associate Professor Jin-Wei Shi (Ed.), ISBN: 978-953-307-277-7, InTech, Available from: <http://www.intechopen.com/books/photodiodes-communications-bio-sensings-measurements-and-high-energy-physics/single-photon-detection-using-frequency-up-conversion-with-pulse-pumping>

**INTECH**  
open science | open minds

### **InTech Europe**

University Campus STeP Ri  
Slavka Krautzeka 83/A  
51000 Rijeka, Croatia  
Phone: +385 (51) 770 447  
Fax: +385 (51) 686 166  
[www.intechopen.com](http://www.intechopen.com)

### **InTech China**

Unit 405, Office Block, Hotel Equatorial Shanghai  
No.65, Yan An Road (West), Shanghai, 200040, China  
中国上海市延安西路65号上海国际贵都大饭店办公楼405单元  
Phone: +86-21-62489820  
Fax: +86-21-62489821

© 2011 The Author(s). Licensee IntechOpen. This chapter is distributed under the terms of the [Creative Commons Attribution-NonCommercial-ShareAlike-3.0 License](#), which permits use, distribution and reproduction for non-commercial purposes, provided the original is properly cited and derivative works building on this content are distributed under the same license.

IntechOpen

IntechOpen